JOURNAL OF VIROLOGY, Apr. 2008, p. 4016–4027 Vol. 82, No. 8
0022-538X/08/$08.00+0 doi:10.1128/JVI.02164-07

Antiviral Therapy during Primary Simian Immunodeficiency Virus Infection Fails To Prevent Acute Loss of $CD4^+$ T Cells in Gut Mucosa but Enhances Their Rapid Restoration through Central Memory T Cells[▽]

David Verhoeven, Sumathi Sankaran, Melanie Silvey, and Satya Dandekar*

Department of Medical Microbiology and Immunology, School of Medicine, University of California, Davis, California

Received 3 October 2007/Accepted 2 February 2008

Gut-associated lymphoid tissue (GALT) is an early target of human immunodeficiency virus (HIV) and simian immunodeficiency virus (SIV) and a site for severe $CD4^+$ T-cell depletion. Although antiretroviral therapy (ART) is effective in suppressing HIV replication and restoring $CD4^+$ T cells in peripheral blood, restoration in GALT is delayed. The role of restored $CD4^+$ T-cell help in GALT during ART and its impact on antiviral $CD8^+$ T-cell responses have not been investigated. Using the SIV model, we investigated gut $CD4^+$ T-cell restoration in infected macaques, initiating ART during either the primary stage (1 week postinfection), prior to acute $CD4^+$ cell loss (PSI), or during the chronic stage at 10 weeks postinfection (CSI). ART led to viral suppression in GALT and peripheral blood mononuclear cells of PSI and CSI animals at comparable levels. CSI animals had incomplete $CD4^+$ T-cell restoration in GALT. In PSI animals, ART did not prevent acute $CD4^+$ T-cell loss by 2 weeks postinfection in GALT but supported rapid and complete $CD4^+$ T-cell restoration thereafter. This correlated with an accumulation of central memory $CD4^+$ T cells and better suppression of inflammation. Restoration of $CD4^+$ T cells in GALT correlated with qualitative changes in SIV gag-specific $CD8^+$ T-cell responses, with a dominance of interleukin-2-producing responses in PSI animals, while both CSI macaques and untreated SIV-infected controls were dominated by gamma interferon responses. Thus, central memory $CD4^+$ T-cell levels and qualitative antiviral $CD8^+$ T-cell responses, independent of viral suppression, were the immune correlates of gut mucosal immune restoration during ART.

With an abundance of activated memory $CD4^+$ T cells in gut-associated lymphoid tissue (GALT), it serves as an early target of human immunodeficiency virus (HIV) and a site of high viral replication (11, 12, 45, 50, 55). Severe depletion of $CD4^+$ T cells in GALT occurs during primary HIV infection that is not reflected in the peripheral blood until the chronic stage of infection (9, 21, 22, 35, 41, 47). In HIV-infected patients receiving antiretroviral therapy (ART), restoration of $CD4^+$ T cells in the GALT is incomplete and protracted compared to the peripheral blood compartment (21, 22). This discordance may be associated with an incomplete suppression of viral replication and persistent inflammation and immune activation in GALT (16–18, 21, 22). The simian immunodeficiency virus (SIV)-infected rhesus macaque model of AIDS provides an excellent opportunity to investigate the dynamics of viral suppression and gut mucosal $CD4^+$ T-cell restoration in controlled experimental settings (16, 24, 43, 51, 65). Like HIV, high viral replication in GALT during primary SIV infection leads to severe $CD4^+$ T-cell depletion, impaired epithelial barrier and nutrient absorptive functions, increased inflammation, and impaired mucosal regeneration (17, 21, 68). Investigations are needed to determine whether mucosal $CD4^+$ T-cell restoration can be enhanced by initiating therapeutic intervention prior to advanced infection and thus achieve better viral suppression and limiting local immune activation in the GALT that can exacerbate $CD4^+$ T-cell loss. It will be important to examine how viral suppression, through early therapeutic intervention, would modulate or impact host immune and inflammatory responses and how they correlate with the magnitude of mucosal immune restoration.

Activated $CCR5^+$ memory $CD4^+$ T cells are major targets of both SIV and HIV and are highly enriched in GALT (9, 35, 41, 70). Central memory (CM) and effector memory (EM) $CD4^+$ T-cell subsets in human and rhesus macaque lymphocyte populations have been identified based on the coexpression of the cell surface markers: CCR7, CD27, CD95, and CD28 (56–59, 67). Unlike peripheral blood, the immunophenotypic characteristics of resident GALT $CD4^+$ T-cell memory subsets in nonhuman primates have been primarily defined based on the use of CD95 and CD28 (53, 57, 58). In humans, immunophenotypic characterization of T-cell subsets has been based on the expression of CCR7, CD28, and CD27 (4, 14, 23). In addition, the immunophenotype of $CD4^+$ T cells restored in GALT during ART has not been fully determined in the SIV model.

In HIV and SIV infections, the majority of virus-specific memory T cells produce gamma interferon (IFN-γ) but not interleukin-2 (IL-2), suggesting a proliferative or functional defect with virus-specific $CD8^+$ T cells reliant on a diminished $CD4^+$ T-cell pool for their supply of IL-2 (23). Polyfunctional virus-specific $CD8^+$ T-cell responses are associated with better viral control than single IFN-γ-expressing cells (33, 60, 73). It

* Corresponding author. Mailing address: Dept. of Medical Microbiology and Immunology, GBSF, Room 5511, University of California, Davis, CA 95616. Phone: (530) 752-3409. Fax: (530) 754-7240. E-mail: sdandekar@ucdavis.edu.

▽ Published ahead of print on 13 February 2008.

is not known whether the functionality of antiviral CD8+ T-cell responses is enhanced in GALT during ART in the context of memory CD4+ T-cell restoration and viral suppression. In addition, the effects of limiting SIV replication very early in infection by starting ART during the acute stage may influence the generation of antiviral CD8+ T cells, and the efficacy of CD4+ T-cell restoration remains to be investigated.

To gain insights into CD4+ T-cell restoration in GALT during therapy, we evaluated memory CD4+ T-cell subsets, viral kinetics, the magnitude of mucosal inflammation, and antiviral CD8+ T-cell responses in SIV-infected rhesus macaques, initiating ART either during the primary (PSI) or chronic (CSI) stage of infection. The initiation of ART at 1 week postinfection (PSI) did not prevent acute CD4+ T-cell loss in GALT during primary SIV infection but supported rapid and complete CD4+ T-cell restoration compared to CSI animals. Our findings suggest that the CD4+ T-cell regeneration capability and not the magnitude of acute CD4+ T-cell loss distinguished the two experimental groups (PSI and CSI). Preservation of central memory CD4+ T cells and suppression of inflammation were associated with better CD4+ T-cell restoration in GALT and led to changes in the qualitative virus-specific CD8+ T-cell responses. These findings highlight the importance of exploring therapeutic strategies that seek to preserve memory, reduce inflammation, and thus promote the mucosal repair and regeneration processes.

MATERIALS AND METHODS

Viral infection and sample collection. Fifteen healthy colony-bred male *Macaca mulatta* animals from the California National Primate Research Center were intravenously infected with 100 animal infectious doses of pathogenic SIVmac251. Two groups of animals were treated with 30 mg/kg of body weight of (*R*)-9-(2-phosphonylmethoxyypropyl)adenine (PMPA) and 30 mg/kg of −2′,3′dideoxy-3′-thia-5-fluorocytindine (FTC). The ART was initiated at either 1 week postinfection ($n = 5$; primary treatment group) or 10 weeks of postinfection ($n = 5$; chronic treatment group) and continued for 30 weeks thereafter. SIV-infected animals without therapy ($n = 5$) served as controls. Jejunal biopsies were collected by upper endoscopy. Jejunal biopsies or 5-cm jejunal resections with mesenteric lymph node biopsy tissue were collected from SIV-infected animals at preinfection and 1 to 2 weeks, 6 to 7 weeks, 16 to 17 weeks, 26 weeks, and 30 to 40 weeks (necropsy) postinfection. Peripheral blood samples were obtained (10 ml) weekly for the first 8 weeks and then biweekly thereafter. Uninfected healthy animals served as negative controls for comparison ($n = 5$).

Cell isolation and flow cytometry. Jejunal biopsies or 5-cm resections were incubated in RPMI 1640 medium (Invitrogen, Carlsbad, CA) and collagenase (Sigma, St. Louis, MO) at 37°C twice for 45 min, and lymphocytes were enriched by Percoll density gradient centrifugation (Sigma). Peripheral blood and lymph nodes were processed as described previously (16). Multicolor immunophenotyping was performed on a modified LSRII (BD, San Jose, CA) with a minimum of 300,000 events collected. Directly conjugated or unconjugated antibodies were obtained from BD Biosciences (San Jose, CA) or eBioscience (San Diego, CA) for the detection of CD3 (SP34)–allophycocyanin (APC)-Cy7, CD4 (OKT4)-Pacific Blue, CD8 (3B5)–APC-Cy5.5, CD69 (FN50)-fluorescein isothiocyanate (FITC), CD95 (DX5)–phycoerythrin (PE)-Cy5, CD28 (CD28.2)–APC-PE-Cy7-Alexa 488, CCR7 (MAB197) with anti-mouse 2a biotin and QDot 605 streptavidin, Ki-67 (MIB-1)–FITC, BRDU (PRB1)-FITC, CD45RA (MEM-56)–PE-Texas Red, CXCR4 (12G5)–PE-Cy7-PE-Cy5, CD25 (BC96)-APC, IL-2 (MQ1-17H12)–FITC, IFN-γ (B27)–PE-Cy7, CD127 (R34.34)-PE, tumor necrosis factor (TNF; MAB11)-PE, CD27 (O323)-APC, and perforin (PF80/164)-Pacific Blue. The data were evaluated by the FlowJo program (TreeStar, Ashland, OR) using doublet discrimination and live amine dyes (Invitrogen).

SIV-specific T-cell responses. Antigen-specific CD8+ T-cell responses were determined in peripheral blood or gut lymphocytes at 6, 16, and 30 weeks posttherapy in SIV-infected animals and in untreated SIV-infected controls using SIVmac251 overlapping gag peptides (NIH AIDS Reference and Research Reagent Program) in an 11-parameter three-cytokine (IL-2, IFN-γ, and TNF-α) flow cytometric assay using a modified LSR II (Becton Dickinson). A minimum of 300,000 events were collected. Briefly, freshly isolated PBMC and GALT T cells were rested overnight in RPMI 10. A total of 1×10^6 T cells were added to 96-well U-bottom plates (Costar) and stimulated with 1 μg/ml each using SIVmac251 overlapping gag peptides (NIH AIDS Reference and Research Reagent Program) with 1 μg/ml anti-CD28 (CD28.2; Pharmingen, San Jose, CA) and 0.5 μg/ml anti-CD49d (9F10; Pharmingen) for 1 h prior to the addition of 10 μg/ml of brefeldin A (Sigma). For positive controls, cells were stimulated with *Staphylococcus aureus* enterotoxin B (SEB). Cells incubated with only medium and antibodies served as negative controls. Cells were stimulated for five more hours and washed with phosphate-buffered saline and antibody-staining fluorescence-activated cell sorting buffer. Cell surface marker staining (clones mentioned above) for CD3–APC-Cy7, CD4-Pacific Blue, CD8–APC-Cy5.5, CD95–PE-Cy5, and CD27–PE-Cy5.5 was performed prior to fixation and Perm washing using 1× BD Fix and Perm solutions. Intracellular staining was performed using IL-2 (MQ1-17H12)–FITC, IFN-γ (B27)–APC, CD69–PE-Cy7, and TNF-α (MAB11)–PE (TNF at 35 to 40 weeks postinfection only). Cytokine-positive gating was set using SEB and medium-only controls with live gating using violet amine dye with doublet discrimination. Flow cytometry was performed within 24 h of antibody staining. Boolean gating and bivariate plots were used to separate cells into categories of specific responses based on single cytokine or polyfunctional cytokine responses. Background from unstimulated controls was subtracted from each sample, and samples with greater than a 0.05% response above background and above the threshold set by SEB controls were considered positive responders. SPICE software (version 3.1; courtesy of Mario Roederer, VRC, NIAID, NIH, Bethesda, MD) was used to illustrate the data.

Measurement of viral RNA loads in plasma and in tissues. SIV RNA loads in plasma and tissue samples were determined by real-time reverse transcription-PCR (RT-PCR) as previously described (25, 34). Plasma viral RNA was extracted from duplicate aliquots and reverse transcribed, and real-time RT-PCR was performed. Fluorescent signal was detected using an Applied Biosystems Prism 7900 sequence detection system, and data were analyzed with Sequence Detector software. Viral RNA copy numbers for experimental samples were determined by plotting C_T values (the fractional cycle number at which the fluorescence passes the fixed threshold for detection) against a regression curve derived from control transcript samples with known SIV copy numbers. This was followed by normalization for the volume of the plasma samples (17). Tissue viral loads were also determined by real-time PCR. Briefly, total RNA was extracted from jejunal tissue. cDNA was synthesized using SuperScript III (Invitrogen) according to the manufacturer's protocol. Five microliters of cDNA was then used in a real-time PCR assay, and the C_T value was plotted against a known standard curve to determine SIV viral RNA copies in the given sample. This value was then normalized for the amount of RNA used in the reaction mixture, and the number of SIV viral RNA copies per μg of total RNA was calculated (44).

Measurement of host gene expression by real-time PCR. Expression of inflammation-associated genes was assessed by real-time PCR from frozen tissue samples. RNA levels of phospholipase A2, pancreatitis-associated protein, transforming growth factor β (TGF-β), tumor necrosis factor alpha, interleukin-8, and macrophage interferon-inducing gene (11, 12, 13) were determined from cDNA and compared as relative expression changes in CSI animals compared to PSI animals. These genes were selected based on our previous studies of SIV-induced changes in gut mucosal gene expression in rhesus macaques (16, 18). These genes were consistently up-regulated in untreated SIV-infected animals (17, 18). Primer-probe pairs specific for the rhesus macaque genes were designed, tested, and validated to have an amplification efficiency of >95%, comparable to that of glyceraldehyde-3-phosphate dehydrogenase (GAPDH). Primers for pancreatitis-associated protein (PAP; HS00170171 ml), PLA2 (Hs00899715 ml), and TGF-β (Hs00171257 ml) were obtained from Applied Biosystems (Foster City, CA). Primers for IL-8 (forward, TGGCTCTCTTGGC AGCCT; reverse, TTGGGGTGGAAAGGTTTGGA; probe, TCTGTGAAGG TGCAGTTTTGCCAAGG), TNF-α (forward, AGGCAGTCAGATCATCTTC TCGAA; reverse, GGAGCTGCCCCTCAGCTT; probe, AGCCTGTAGCCCA TGTTGTAGCAAACCCT), and prGAPDH (forward, GCACCACCAACTGC TTAGCACC; reverse, TCTTCTGGGTGGCAGTGATG; probe, TCGTGGGA AGGACTCATGACCACAGTCC) were designed, optimized, and validated for use by the Lucy Whittier Molecular Core Lab (University of California, Davis). Relative cytokine mRNA expression levels were calculated from normalized ΔC_T (cycle threshold) values and are reported as the change. C_T values correspond to the cycle number at which the fluorescence signal exceeds the background fluorescence (threshold). In this analysis, the C_T value for the housekeeping gene (GAPDH) was subtracted from the C_T value of the target gene for each sample for normalization. The target gene and the reference gene (GAPDH) amplified

with the same efficiency (data not shown). For the detection of changes in gene expression in SIV-infected untreated animals or in PSI and CSI animals, the RNA levels for each gene in the CSI and PSI animals and untreated controls were compared with the levels in the SIV-negative healthy controls (calibrator), and data are presented as the change in expression of each gene. The ΔC_T value for the tissue sample from the calibrator was then subtracted from the ΔC_T value of the corresponding tissue sample from the CSI animal ($\Delta\Delta C_T$). The increase in cytokine mRNA levels in jejunal tissue samples of the CSI animals compared to tissue samples of baseline (calibrator) animals was then calculated as follows: increase = $2^{\Delta\Delta CT}$ (user bulletin 2; ABI Prism 7700 Sequence Detection System; Applied Biosystems).

To determine the magnitude of difference in gene expression levels between the PSI and CSI groups, the data are presented as a ratio of the CSI to PSI. The PSI sample was used as the calibrator in this analysis (1, 62).

Western blot analysis. Levels of stress response-related proteins in gut biopsies of SIV-infected animals and uninfected controls were evaluated by Western blot analysis. Protein extracts were prepared from frozen tissue by resuspending in phosphate-buffered saline–1% Triton–phenylmethylsulfonyl fluoride and sonicating twice in 4-s bursts. Antibodies to glucose response protein 78 and heat shock protein 78 (Santa Cruz Biotechnology, Santa Cruz, CA) were used on the Western blots and calibrated with anti-GAPDH (Santa Cruz Biotechnology) on the same gel.

Statistical analysis. Statistical analysis was performed using the program Minitab (Minitab Inc., State Park, PA). The significance of the differences between control (SIV-infected untreated animals) and experimental (SIV-infected animals who receive ART) groups of animals was determined using the Mann-Whitney U test, and P values of <0.05 were considered significant.

RESULTS

Suppression of SIV replication in PSI and CSI during ART. To investigate whether initiating ART early in infection would determine the magnitude of viral suppression in the peripheral blood and GALT, we analyzed longitudinal samples of plasma and jejunum samples from animals initiating ART at 1 week postinfection (PSI group) or at 10 weeks postinfection (CSI group) in comparison to SIV-infected animals that were therapy naïve. The beginning of plasma viral load suppression was observed within 1 week of starting ART (2 weeks postinfection) in the PSI animals (average, 3.2×10^4 RNA copies/ml), while plasma viral loads reached 5×10^6 to 11.3×10^6 RNA copies/ml in CSI animals as well as in untreated controls at 2 weeks postinfection (Fig. 1A). Both PSI and CSI showed a decline in viral loads after the initiation of ART that continued to drop during treatment (<100 copies at 32 weeks postinfection), while viral RNA copy numbers reached a steady set point in the untreated controls after 10 weeks postinfection (average, 5.1×10^5 copies/ml) that persisted through the course of infection.

Measurement of viral RNA levels in GALT at 6, 16, and 30 weeks of therapy showed that there was a substantial decline ($P < 0.05$) in the viral loads at 6 weeks posttherapy (Fig. 1B) in both PSI (average, 3.2×10^3 SIV copies per μg of total RNA) and CSI (average, 3.6×10^2 copies) groups compared to the untreated SIV-infected group (average, 2.4×10^6 copies). Viral RNA levels continued to remain lower in both PSI and CSI groups ($P < 0.05$) at 16 weeks (PSI, 2.1×10^3 copies; CSI, 1.3×10^3 copies) and 30 weeks (PSI, 2.3×10^3 copies; CSI, 3.0×10^3 copies) of therapy compared to untreated SIV-infected controls (1 week postinfection, 6.0×10^3; 16 weeks postinfection, 5.2×10^5; 30 weeks postinfection, 5.7×10^5) (Fig. 1B). In general, the level of viral suppression in GALT was comparable between the PSI and CSI groups during ART. However, although plasma viral loads were below detection limits by 32 weeks postinfection in both PSI and CSI animals, complete suppression of viral RNA loads in GALT was not achieved.

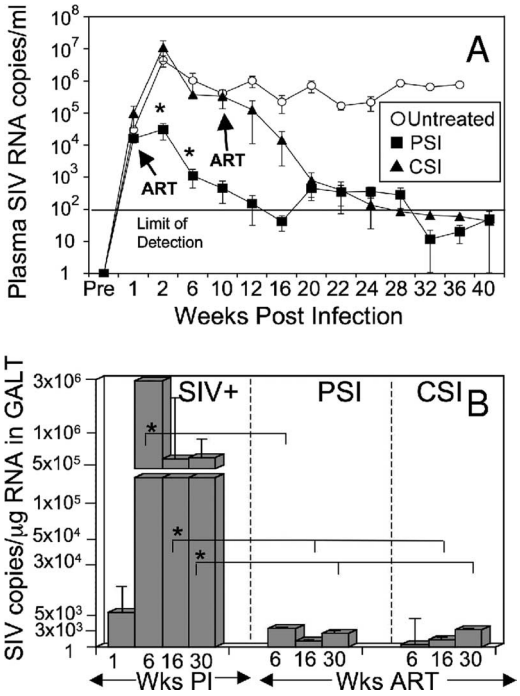

FIG. 1. Initiation of combination ART leads to viral suppression in plasma and GALT of SIV-infected rhesus macaques compared to untreated controls. (A) Plasma viral loads were measured by real-time PCR in untreated SIV^+ animals, PSI animals (initiating ART at 1 week postinfection), and CSI animals (initiating ART at 10 weeks postinfection). Arrows indicate the time of the initiation of ART. (B) Viral RNA loads in GALT of untreated SIV^+ controls and PSI and CSI animals were determined by real-time PCR. Viral loads were calculated based on SIV copies per μg of total tissue RNA (mean ± standard error; $n = 5$ for each group). The level of detection was 200 SIV copies per μg of total tissue RNA. The dotted lines indicate the level of detection of SIV RNA copies. Asterisks indicate statistically significant differences between PSI and CSI groups and between PSI and untreated controls ($P < 0.05$) at the indicated time points.

Magnitude of $CD4^+$ T-cell restoration in PSI and CSI animals. A progressive loss of $CD4^+$ T cells was seen in the peripheral blood of untreated SIV-infected animals (Fig. 2A). Despite the start of therapy at 1 week postinfection, the PSI group experienced a gradual decline in $CD4^+$ T cells in the peripheral blood until 6 weeks postinfection, followed by a period of recovery (Fig. 2A). After 26 weeks of ART, complete restoration of $CD4^+$ T-cell numbers to preinfection baseline values (885 to 1,420 $CD4^+$ T cells/mm^3) was achieved in the PSI animals (1,008 to 1,335/mm^3). The CSI animals also showed a gradual loss in circulating $CD4^+$ T-cell numbers following SIV infection (55% reduction compared to preinfection values). A rebound in $CD4^+$ T-cell numbers was detected after 6 weeks of ART that continued to increase during therapy.

In GALT, untreated SIV-infected animals showed severe depletion of $CD4^+$ T cells at 2 weeks postinfection that was sustained thereafter (Fig. 2B). On average, about 50% of the $CD4^+$ T cells in GALT were depleted at 1 week postinfection and >80% at 2 weeks postinfection. It was notable that the

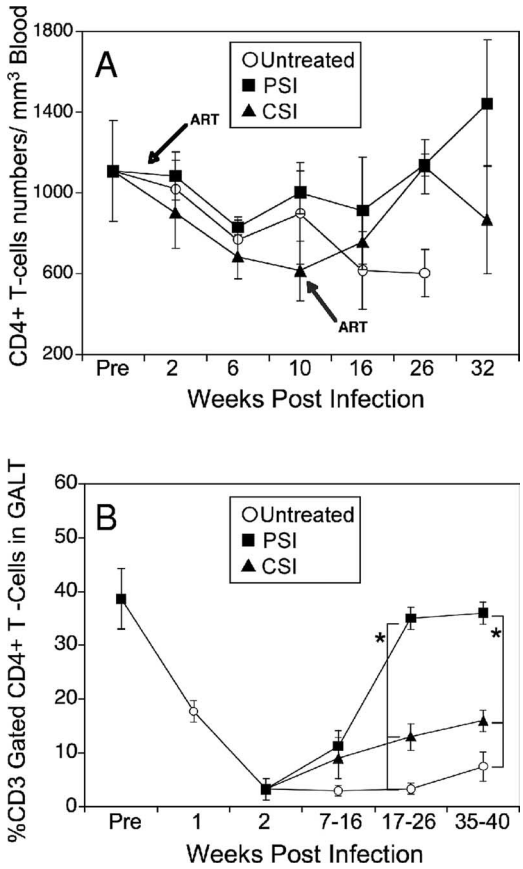

FIG. 2. Full restoration of $CD4^+$ T cells in GALT of SIV-infected animals starting ART during acute SIV infection. Longitudinal samples of peripheral blood (A) and GALT (B) were obtained from PSI and CSI animals and untreated SIV^+ controls. The $CD4^+$ T-cell counts or percentages were determined by flow cytometric analysis (mean ± standard error; $n = 5$ in each group). Asterisks indicate statistically significant differences between PSI and CSI groups and between PSI and untreated controls ($P < 0.05$) at the indicated time points.

initiation of ART in the PSI group at 1 week postinfection did not prevent this severe loss of $CD4^+$ T cells during the primary acute phase at 2 weeks postinfection (average, 8% of total $CD3^+$ T cells), which was similar to that seen in untreated SIV-infected animals (average, 5% of total $CD3^+$ T cells). However, there was an accelerated restoration of intestinal $CD4^+$ T cells in the PSI animals that was not observed in the CSI animals. After 16 weeks of ART, three of the five PSI animals restored $CD4^+$ T cells to at least 95% of preinfection levels ($P < 0.05$ for comparison between CSI and untreated controls). After 30 weeks of ART, all animals in the PSI group had repopulated $CD4^+$ T cells in GALT to preinfection levels and had a completely divergent pattern of restoration from the CSI ($P < 0.05$). In contrast, the CSI group displayed modest restoration of $CD4^+$ T cells in GALT after 16 weeks of ART (13% $CD4^+$ T cells in GALT compared to 40% at the preinfection time point) and only a modest increase after 30 weeks of ART (~15% $CD4^+$ T cells). The CSI group showed a positive trend of gradual but slow restoration of gut $CD4^+$ T cells compared to untreated controls. Our data suggested that the timing of the initiation of ART influenced the magnitude and time course of restoration of $CD4^+$ T cells in GALT and was independent of the acute $CD4^+$ T-cell loss.

$CD4^+$ T-cell repopulation in PSI animals is driven through central memory and transitional memory $CD4^+$ T-cell subsets. To characterize the $CD4^+$ T-cell subsets that were lost during infection, we performed multicolor flow cytometric analysis of T-lymphocyte populations from uninfected healthy controls (Fig. 3). A majority of the $CD4^+$ T cells in GALT expressed CD95, CD28, CCR7, and CD27 and had an immunophenotype very similar to that of human central memory $CD4^+$ T cells, defined as $CD95^+$ $CD28^+$ $CD27^+$ $CCR7^+$ (Fig. 3). In addition, these CM $CD4^+$ T cells expressed Ki-67 (Fig. 3) and produced IL-2 in response to SEB stimulation (data not shown). However, only approximately 60% of this population expressed the CCR7 coreceptor, indicating that the remaining cells might have been transitioning to the effector memory phenotype and are defined as $CD95^+$ $CD27^+$ $CD28^+$ $CCR7^-$. These cells also produced IL-2 and IFN-γ upon SEB stimulation. Effector memory $CD4^+$ T cells, defined as $CD95^+$ $CD28^-$ $CD27^-$ $CCR7^-$, comprised a minor fraction (4 to 6%) of the total $CD4^+$ T cells in GALT of uninfected healthy controls. Upon stimulation with SEB, this T-cell population produced IFN-γ (45% of EM $CD4^+$ T cells) and perforin (3% of EM $CD4^+$ T cells), suggesting that they had effector memory functions. In summary, the majority of $CD4^+$ T cells in GALT of uninfected healthy rhesus macaques were of CM and transitional CM phenotypes.

To evaluate changes in the memory $CD4^+$ T-cell subsets in GALT during SIV infection and following the start of therapy, we performed immunophenotypic characterization of intestinal T cells in the PSI, CSI, and untreated SIV-infected animals by utilizing multicolor flow cytometry. In all SIV-infected animals, a severe loss of effector memory $CD4^+$ T cells occurred during primary SIV infection compared to uninfected controls (Fig. 4A) that was evident by 6 weeks postinfection (data not shown) and continued to 30 weeks of infection (Fig. 4B). Furthermore, the pool of proliferating central memory cells, detected as $Ki\text{-}67^+$ cells, was lower (average, 3% of total $CD4^+$ T cells) in SIV-infected animals within 1 week of infection compared to uninfected controls (6%) (data not shown). Thus, SIV infection led to changes in the proliferative T-cell pool that may have led to a reduction in the total central memory pool by possibly increasing the rate of activation/differentiation-associated cell death. In the PSI animals, restoration of $CD4^+$ T cells (95% of preinfection values) in GALT was achieved within 16 weeks of therapy, and these cells were mainly comprised of the CM (60 to 67%) and transitional CM phenotypes (Fig. 4D). A rebound in the transitional memory $CD4^+$ T cells observed at 16 weeks of therapy (9 to 13% compared to 1 to 3% at 6 weeks of ART) suggests that CM subsets might have been differentiating into the effector cells at an increased rate (Fig. 4D). In contrast to PSI animals, CM $CD4^+$ T cells in CSI animals were detected at lower levels ($P < 0.05$) at 16 weeks of ART (Fig. 4C). At 30 weeks of therapy, $CD4^+$ T-cell subsets in GALT of both PSI and CSI animals were comprised of CM, transitional CM, and EM. However, the percentage of CM (38% in PSI and 50% in CSI) was lower compared to uninfected controls, and an increased accumulation of transitional CM was observed in both groups. Overall,

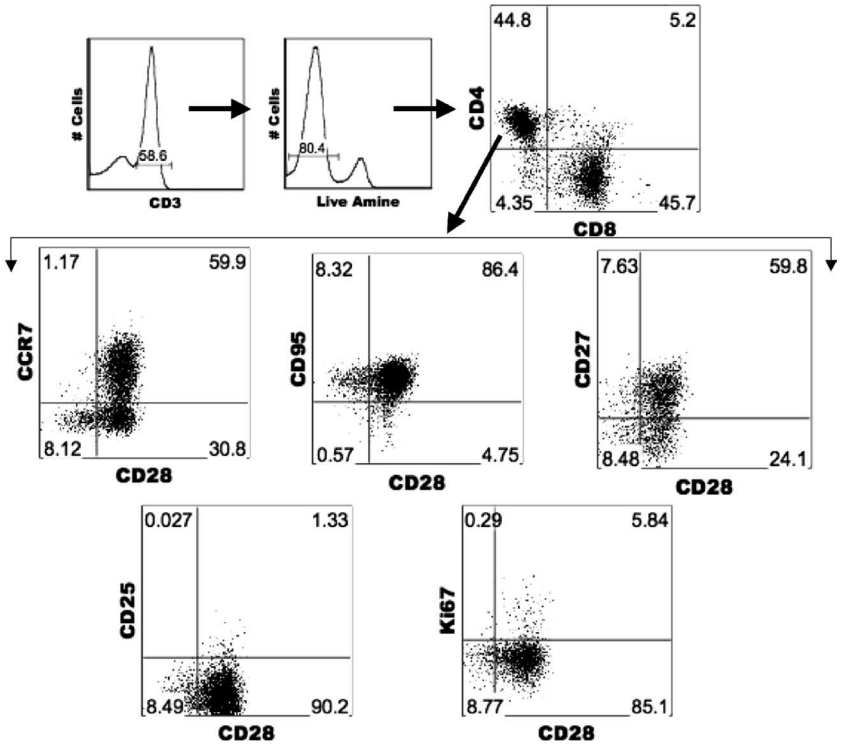

FIG. 3. The $CD4^+$ T cells in GALT are comprised of central memory cells, effector memory cells, and an intermediate population. Flow cytometric analysis of isolated mononuclear cells from the GALT of uninfected rhesus macaques was performed by gating on live cells and CD3 along with doublet discrimination. $CD4^+$ T cells were then forward gated, showing percentage that express CCR7/CD28, CD95/CD28, CD27/CD28, CD25/CD8, and Ki-67/CD28. A representative animal from the uninfected control group is shown ($n = 5$).

the PSI displayed higher ($P < 0.05$) percentages of effector memory cells than the CSI group at 16 weeks (PSI, 8.1 to 12.2% of total $CD4^+$ T cells; CSI, 0 to 2%) and 30 weeks (PSI, 17.3 to 21.4%; CSI, 3.3 to 6.4%) of ART (Fig. 4E and F, respectively).

The percentage of CM $CD4^+$ T cells in peripheral blood continued to decline in the untreated controls, reaching 3 to 5% of total $CD4^+$ T cells by 40 weeks postinfection. The beginning of CM $CD4^+$ T-cell restoration (10 to 15% of total $CD4^+$ T cells) in peripheral blood of both PSI and CSI animals was observed at 6 weeks of ART. Throughout the course of ART, the percentage of CM $CD4^+$ T cells continued to increase in both PSI and CSI groups, peaking at 20 to 28%, which closely resembled preinfection values.

Qualitative changes in SIV-specific $CD8^+$ T-cell responses in GALT during ART. To investigate whether the magnitude of the restoration of $CD4^+$ T-cell help in GALT influenced SIV-specific cellular responses, we evaluated anti-SIV $CD8^+$ T-cell responses in PSI and CSI animals during ART by intracellular cytokine staining using overlapping SIV gag peptides. In untreated SIV-infected controls, SIV-specific $CD8^+$ T-cell responses in GALT were dominated by single IFN-γ production at 6 weeks postinfection (average, 0.23% of total $CD8^+$ T cells). The IFN-γ-producing responses continued to increase during the course of SIV infection, with the highest level detected at 30 weeks of infection (0.9%), as shown in Fig. 5A and B. The second highest response was of dual IFN-γ/IL-2-producing $CD8^+$ T cells, which was detected at 16 weeks postinfection (0.15%) and 30 weeks postinfection (0.12%). These data suggested that polyfunctional responses (dual IFN-γ/IL-2) were found in the later stages of infection, possibly driven in response to high viral antigen load. Since polyfunctional $CD8^+$ T-cell responses are considered to be more effective in viral control than single IFN-γ-producing cells, their absence in GALT during early infection may partly contribute to inefficient control of SIV infection as observed in the GALT of untreated controls.

In the PSI animals, single IFN-γ-producing $CD8^+$ T-cell responses in GALT were seen at 6 weeks postinfection (0.07%), while we observed single IL-2- or IFN-γ-producing $CD8^+$ T-cell responses at 17 weeks postinfection (16 weeks of ART). While polyfunctional responses ($IL\text{-}2^+$ $IFN\text{-}\gamma^+$) were detected at 30 to 40 weeks postinfection (0.095%), the majority of the SIV gag-specific $CD8^+$ T-cell responses were comprised of single IL-2 production at 16 weeks (0.23%) and 30 weeks of ART (0.72%) in the PSI group. In contrast, the CSI animals developed higher levels of single positive (IFN-γ, 0.72%) and polyfunctional CD8 T-cell (IFN-γ/IL-2, 0.14%) responses to SIV antigens at 16 weeks of therapy than the PSI group, which persisted at 30 weeks of ART (IFN-γ, 0.87%; IFN-γ/IL-2, 0.29%) (Fig. 5A). The magnitude of single IFN-γ-positive responses in CSI was lower compared to the untreated SIV-infected animals, but the levels of polyfunctional responses were similar at 30 weeks of ART.

The antigen-specific responses in the peripheral blood showed trends similar to those observed in the GALT (data not shown). We observed that the generation and dominance of SIV gag-specific IFN-γ-producing $CD8^+$ T-cell responses in

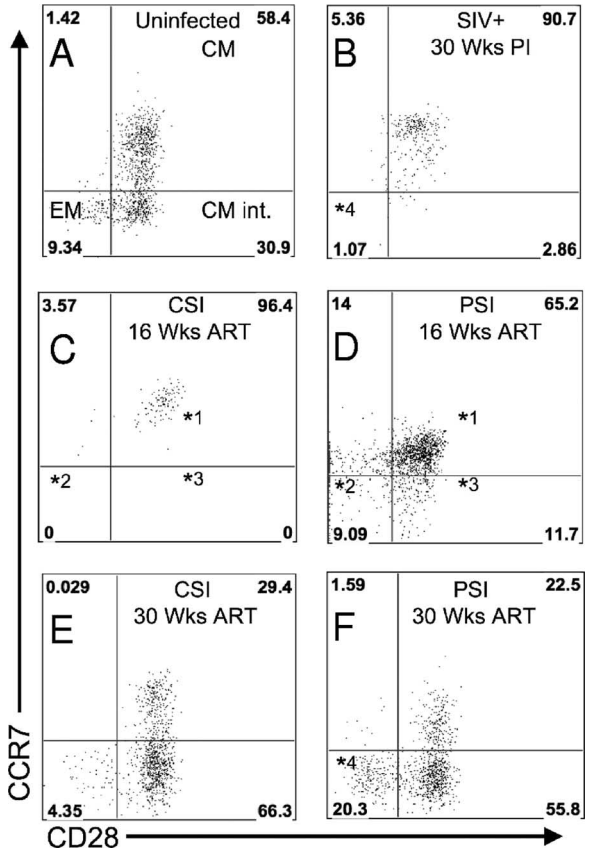

FIG. 4. Early restoration of central memory CD4+ T cells in GALT leads to enhanced gut mucosal CD4+ T-cell restoration during therapy. Flow cytometric analysis was performed to identify memory CD4+ T-cell subsets in GALT, and data are presented for a representative animal from each experimental group. (A) Uninfected healthy control; (B) SIV-infected therapy-naïve animal at 30 weeks postinfection; (C) CSI animal after 16 weeks of ART; (D) PSI animal after 16 weeks of ART; (E) CSI animal after 30 weeks of ART; (F) PSI animal after 30 weeks of ART. Asterisks indicate statistically significant differences between PSI and CSI groups for the memory subsets ($P < 0.05$). Numbers next to asterisks indicate corresponding time points that are significant.

the untreated SIV-infected controls at 6 weeks postinfection (0.08 to 0.11%) and thereafter (0.11 to 0.77%). Polyfunctional responses were not detected in the untreated animals, but single TNF-α-producing responses were present (0.093 to 0.15%). The PSI group had single IL-2-producing CD8+ T-cell responses at 16 weeks of ART (0.06 to 0.99%) that were sustained at 30 weeks of ART (0.22 to 0.44%). Single IFN-γ-producing responses were also elevated (0.05 to 0.44%) after 30 weeks of ART. Single TNF-α responses were detected in 4 of the 5 PSI animals after 30 weeks of therapy (0 to 0.33 in all five animals). In the CSI group, IFN-γ- or TNF-α-producing CD8+ T-cell responses dominated at 6 (IFN-γ, 0.09 to 0.12%; TNF-α, 0.065 to 0.11%), 16 (IFN-γ, 0.05 to 0.13%; TNF-α. 0.07 to 0.09%), and 30 weeks of ART (IFN-γ, 0.075 to 0.19%; TNF-α, 0.0 to 0.088%), with a smaller polyfunctional response of IL-2/IFN-γ at 16 weeks (0.05 to 0.075%) and 30 weeks (0 to 0.081%) of ART. These data suggested that the CD8+ T-cell responses in PBMC mirrored the responses observed in the GALT with respect to IFN-γ responses but were less comparable with single TNF-α-producing responses and polyfunctional responses.

To further determine whether CD8+ T-cell populations in the GALT showed differences in chemokine receptor expression and the type of effector response to viral infection, we evaluated the expression of CCR5 and CXCR4 (Fig. 5C). The CD8+ T cells from GALT of uninfected controls were both singly CCR5 positive (averaging 35%) or dual positive for CCR5 and CXCR4 (averaging 54%). In SIV-infected untreated controls, we observed a shift toward CCR5-expressing CD8+ T cells (68%) without CXCR4 expression as early as 6 weeks postinfection that persisted throughout infection. In the PSI group, we observed that by 16 weeks of ART, there was an accumulation of CCR5 and CXCR4 dual-positive CD8+ T cells in GALT (74.5%) that remained in the GALT at 30 weeks of ART (76.2%), with a smaller fraction of CD8+ T cells expressing CCR5 singly (19.5%). The CSI group had an almost equal proportion of CD8+ T cells with single CCR5 or dual CCR5 and CXCR4 expression at 16 weeks of ART (51.2% CCR5, 48.2% dual) that persisted at 30 weeks of ART (49% CCR5, 46.5% dual). These data suggest that the type of antiviral response was quite different in the PSI group and may have helped to enhance the CD4+ T-cell restoration.

CD8+ T-cell proliferative responses correlated with viral loads and not with the induction of SIV-specific IL-2-producing responses. To investigate the role of CD8+ T-cell proliferation with respect to viral loads and the generation of antigen-specific responses, we determined Ki-67 expression of CD8+ T cells in uninfected controls and compared them with those in ART-naïve SIV-infected animals (at 1 and 30 weeks postinfection) and with the PSI and CSI groups. A low level of proliferation (0.65 to 1.5% of total CD3+ CD8+ PBMC and 0.76 to 2.1% of total CD3+ CD8+ GALT) was seen in the CD8+ T cells of uninfected controls (Fig. 6A). We did not detect any change in the proliferation in CD8+ T cells of ART-naïve SIV-infected controls at 1 week postinfection in either PBMC or GALT, suggesting that mobilization of CD8 responses had not started at that time point (Fig. 6B). However, within 30 weeks of infection, elevated proliferation of GALT CD8+ T cells (8.5 to 15.4%) was observed (Fig. 6C). We found that 2.5 to 4.5% of GALT CD8+ T cells were Ki-67 positive at 16 weeks of ART in the PSI group (data not shown). The level of proliferation was lower (1.5 to 2.3%) at 30 weeks of ART (Fig. 6D) and was significantly different from the SIV-infected untreated controls ($P < 0.05$). The CSI group had higher levels of CD8+ T-cell proliferation than the PSI group at 16 weeks of ART (6.5 to 7.5% in GALT; not statistically significant). The CSI group continued to show higher levels of proliferation at 30 weeks of ART (5.8 to 7.4% in GALT) (Fig. 6E) but was not significantly different than untreated SIV-infected controls or the PSI group. These data suggest that CD8+ T-cell responses were vastly different in the PSI animals in that they displayed continued viral suppression despite decreased proliferative responses.

Early control of intestinal inflammation is associated with improved CD4+ T-cell restoration in GALT. To determine the potential impact of local inflammation on the kinetics of the CD4+ T-cell restoration in GALT, we compared the expression of inflammation-associated genes in PSI and CSI animals

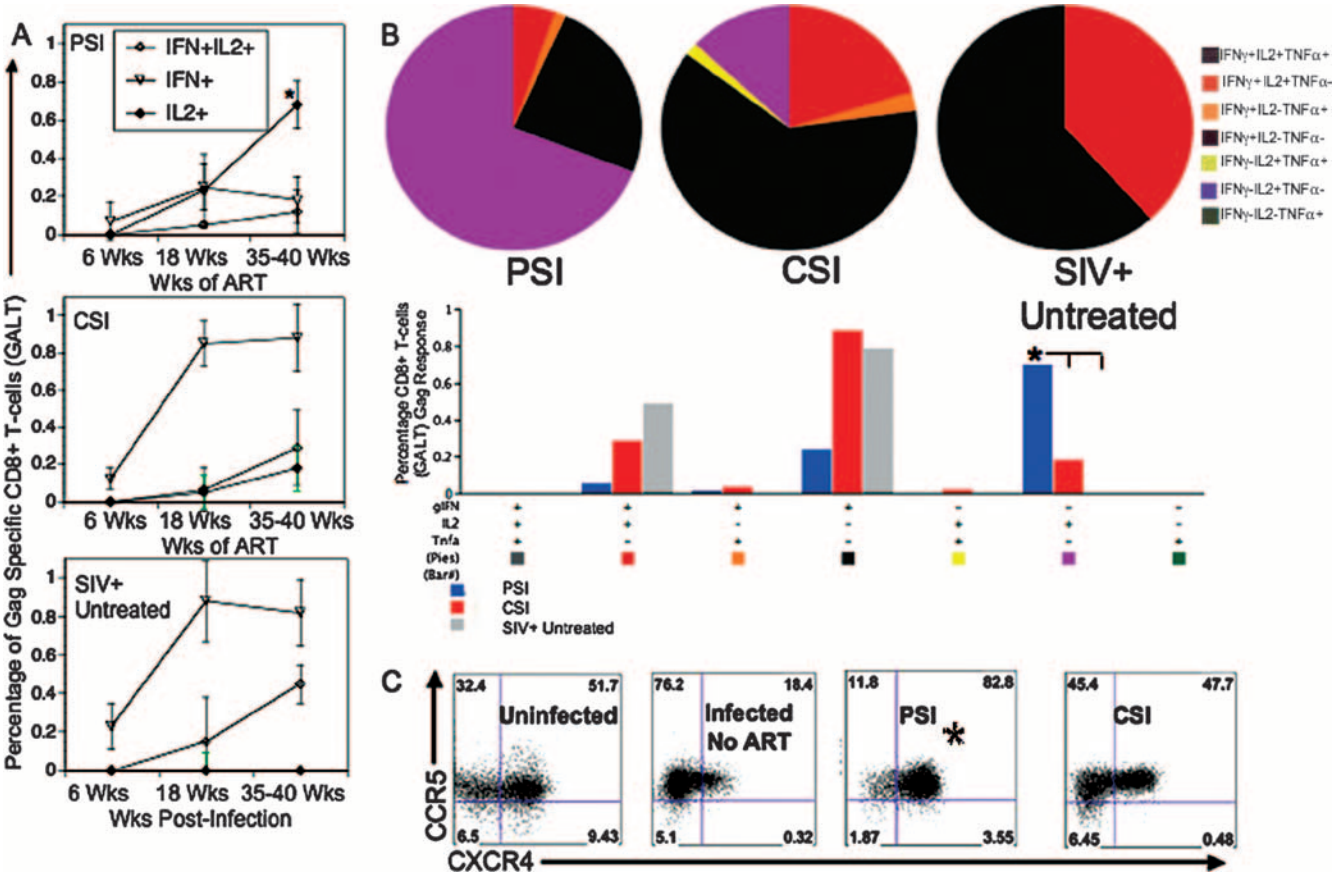

FIG. 5. SIV antigen-specific $CD8^+$ T-cell responses in GALT of SIV-infected rhesus macaques. (A) Longitudinal analysis of SIV gag-specific $CD8^+$ T-cell responses in GALT was performed in SIV-infected therapy-naïve controls and PSI and CSI animals during therapy. Intracellular cytokine responses (IL-2 and IFN-γ) were measured by flow cytometry, and the percentages of SIV gag-specific $CD8^+$ T cells are presented at different time points postinfection or during ART. (B) The functional composition of the SIV-specific $CD8^+$ T-cell responses, showing every possible combination of responses (TNF-α, IL-2, and IFN-γ) after 30 weeks of ART (PSI and CSI) or 30 weeks of infection (SIV^+ untreated), is shown on the *x* axis of the bar graph. Bars indicate the percentages of total SIV gag response contributed by $CD8^+$ T cells with a given functional response. The data are summarized in pie charts, in which each slice represents the fraction of the $CD8^+$ T-cell response for each cytokine singly or in combination. (C) Flow cytometric analysis of the expression of CCR5 and CXCR4 was performed on GALT $CD8^+$ T cells from uninfected, ART-naïve infected controls (30 weeks postinfection), PSI (after 30 weeks of ART), and CSI animals (30 weeks of ART). Data for a representative animal from each group are shown. Asterisks indicate statistically significant differences between PSI and CSI $CD8^+$ T-cell responses and untreated SIV-infected controls ($P < 0.05$) or significant differences in the percentages of both $CCR5^+$ and $CCR5^+$ $CXCR4^+$ $CD8^+$ T cells in the PSI group compared to all other groups.

at 6, 16, and 30 weeks of ART. CSI animals displayed significantly higher levels (average of 13-fold increased expression over PSI animals) of gene expression for PAP, macrophage interferon-inducing gene (MIG; 3.7-fold increase), and TNF-α (3.7-fold increase) than PSI animals after 6 weeks of ART (Fig. 7A). By 16 weeks of ART, CSI animals had higher expression of MIG (2-fold increase), TGF-β (16.5-fold increase), and TNF-α (2.4-fold increase). After 30 weeks of ART, CSI animals had higher expression of PAP (120-fold increase), TGF-β (16.5-fold increase), TNF-α (3.6-fold increase), and IL-8 (2.23-fold increase). Except in PSI animals at 18 weeks of ART, inflammatory genes were always higher in all groups and at all time points than in healthy uninfected controls (data not shown). However, the magnitude of the inflammation was substantially lower in PSI and CSI groups at 30 weeks of ART than the untreated SIV-infected control group at 30 weeks postinfection (Fig. 7B). In addition, CSI animals had increased levels of inducible stress-related proteins (HSP-70 and GRP-78) compared to PSI animals at 30 weeks of ART (Fig. 7C). Thus, comparison of PSI and CSI groups showed that restoration of gut $CD4^+$ T cells correlated with early suppression of inflammation in the gut microenvironment.

DISCUSSION

We have investigated the effects of initiating ART in SIV-infected animals (PSI) during primary SIV infection, prior to the occurrence of acute $CD4^+$ T-cell loss in GALT, which is a characteristic feature of primary viral infection with pathogenic SIV. Data on the $CD4^+$ T-cell restoration were compared with those from the animals starting therapy during chronic SIV infection (CSI). We utilized the PSI group to assess whether intervention prior to the development of severe enteropathic changes in the intestinal microenvironment would alter the magnitude and time course of $CD4^+$ T-cell replenishment. We found that the $CD4^+$ T-cell restoration was

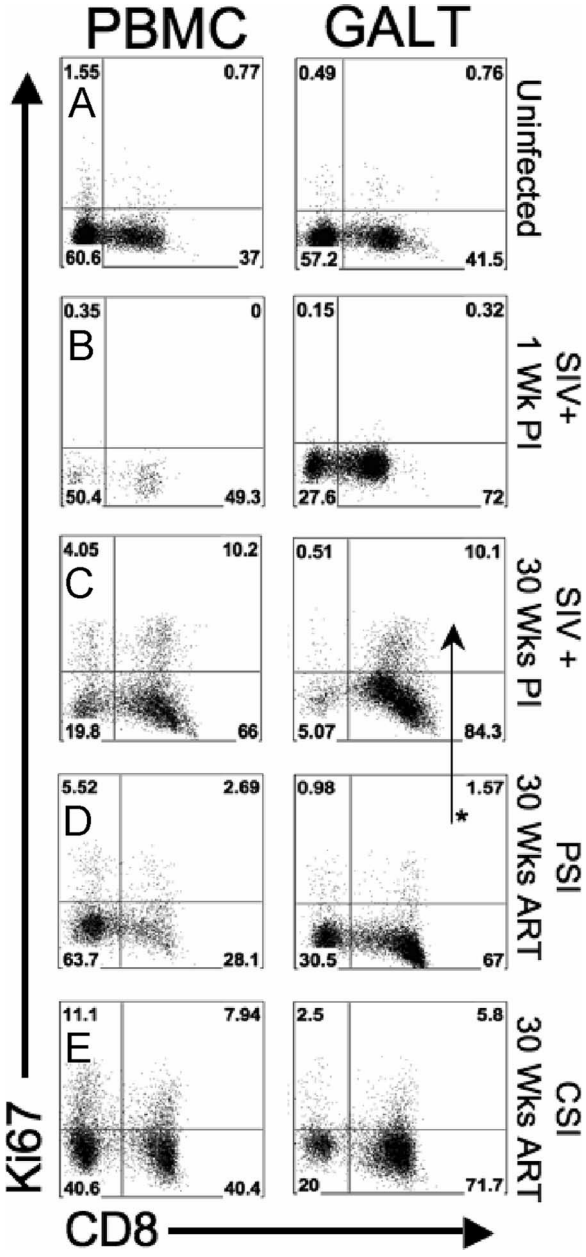

FIG. 6. Proliferation of $CD8^+$ T cells in GALT and peripheral blood of SIV-infected rhesus macaques during ART. Proliferative potential was measured by flow cytometry by gating on Ki-67$^+$ $CD8^+$ T cells of PBMC and GALT of uninfected healthy controls (A), ART-naïve SIV-infected controls at 1 week postinfection (B), ART-naïve SIV-infected controls at 30 weeks postinfection (C), PSI animals at 30 weeks of ART (D), and CSI animals at 30 weeks postinfection (E). Data from a representative animal are shown. The asterisk marks a statistically significant difference in the percentage of proliferating $CD8^+$ T cells ($P < 0.05$).

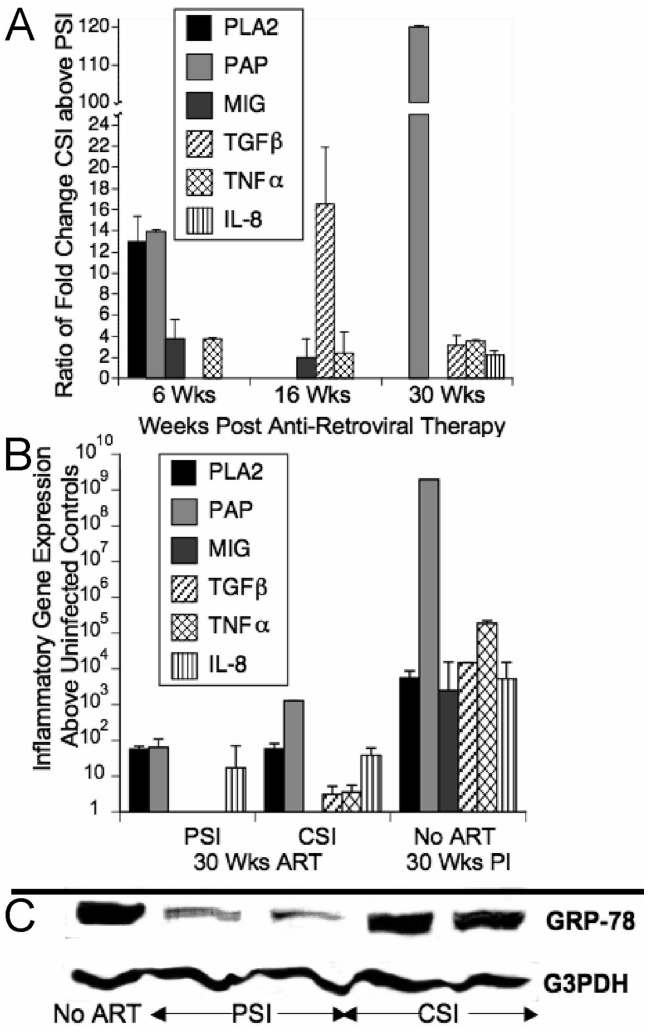

FIG. 7. Suppression of intestinal inflammation correlates with gut mucosal $CD4^+$ T-cell restoration during ART. (A) Intestinal inflammation was assessed by measuring inflammation-associated gene expression (phospholipase A2 [PLA2], PAP, TGF-β, TNF-α [TNFA], IL-8, and MIG) by real-time PCR. To demonstrate the magnitude of the difference between CSI and PSI groups, the ratio of the fold change of CSI over PSI is shown for each gene at various time points, with baseline levels of each gene derived from uninfected controls subtracted from both PSI and CSI averages. (B) An increase in expression of inflammation-associated genes was detected in PSI animals (30 weeks ART), CSI animals (30 weeks ART), and untreated SIV-infected controls (30 weeks postinfection [PI]) by comparison with the baseline values from uninfected healthy controls. (C) A Western blot analysis showed the change in protein levels of glucose response protein 78 (GRP-78) in GALT of PSI and CSI animals at 30 weeks of ART compared to SIV^+ therapy-naïve controls at 30 weeks postinfection.

influenced by the extent of viral suppression, levels of the central memory T-cell subset, and the magnitude of inflammation in the GALT. These data demonstrated that initiation of ART early in infection could lead to rapid and enhanced intestinal $CD4^+$ T-cell repopulation in GALT despite severe depletion during primary SIV infection. Although the initiation of highly active ART (HAART) during primary HIV infection may be difficult if not impractical, our study highlights potential immune and molecular correlates of better GALT restoration that could be useful in the evaluation of vaccines and therapeutics. Our findings also demonstrate that early suppression of viral loads by ART modulate host mucosal responses during infection.

Our previous studies showed that suppression of viral replication correlated with increased $CD4^+$ T-cell repopulation of GALT in HIV and SIV infections during therapy (16, 22). Our findings in the present study suggest that suppression of plasma viral loads occurred after 6 weeks of ART in both PSI and CSI animals, independent of the time of ART initiation, and coincided with increased circulating $CD4^+$ T-cell numbers. However, the magnitude of $CD4^+$ T-cell restoration in GALT of PSI and CSI animals was very different following the start of therapy. Interestingly, SIV-infected $CD4^+$ T cells were depleted at 2 weeks postinfection in PSI animals despite the initiation of ART at 1 week postinfection. This depletion may have resulted because the antiretroviral regimen included reverse transcriptase inhibitors only, which prevented new infections but did not protect the previously SIV-infected cells from virus-mediated cell death. The $CD4^+$ T-cell depletion very closely mirrored previous studies showing that despite early ART, peripheral blood $CD4^+$ T cells were still lost (37, 65). Lifson et al. reported that animals that initiated ART by 24 h of SIVmac239 infection did not experience $CD4^+$ T-cell depletion in GALT (36). The suppression of viral replication immediately following the infection might have prevented massive GALT $CD4^+$ T-cell infection in these animals. In our study, PSI animals started therapy at 1 week postinfection with the highly pathogenic strain SIVmac251, by which time the initial burst of active viral replication and spread of infection could have already occurred. The restoration of the gut $CD4^+$ T cells in the PSI animals after early ART initiation not only modulated immune responses but also controlled the rampant inflammatory conditions, thereby driving better immune restoration.

We determined that the majority of the $CD4^+$ T cells in GALT of uninfected healthy animals were $CD95^+$ $CD28^+$ $CD27^+$ $CCR7^+$ and identified as central memory T cells according to previous definitions (4, 29, 30, 57). However, 30 to 40% of these "central" memory cells had down-regulated CCR7, suggesting that they could represent an intermediate phenotype, transitioning between central memory and effector phenotypes (2, 10, 56, 58). Since the majority of $CD4^+$ T cells in the GALT express CCR5 mRNA but not necessarily CCR5 protein (9), we propose that the rhesus GALT contains two transitional central memory intermediates ($CCR7^+$ $CD28^+$ $CD27^+$, which may be $CCR5^{+/-}$, and $CCR7^-$ $CD28^+$ $CD27^+$, which may be $CCR5^{+/-}$) and fully differentiated effector memory ($CCR7^-$ $CD28^-$ $CD27^-$ $CCR5^+$). The earliest transitional $CD4^+$ T cells ($CCR7^+$ $CD28^+$ $CD27^+$) would be more like central memory and thus more protected from SIV infection, as observed in this study. Further analysis of the CCR5 expression of these three $CD4^+$ T-cell populations is warranted. Since central memory feeds the effector memory pool in lungs, the presence of this differentiating T-cell subset ($CCR7^+$ $CD28^+$ $CD27^+$ $CCR5^{+/-}$) in GALT is not surprising (40). In SIV-infected animals, a severe loss of effector memory $CD4^+$ T cells was seen in GALT as early as 1 week postinfection during the primary infection stage. In addition, a loss from SIV-infected animals of the Ki-67^+ CM $CD4^+$ T-cell pool, present in uninfected healthy macaques, was observed and suggests that CM cells were either rapidly transitioning to an EM phenotype and subsequently depleted by infection or were lost as CM due to their proliferative state (52, 71).

An increase in central memory $CD4^+$ T cells was observed in both PSI and CSI animals after 30 weeks of ART compared to untreated SIV^+ animals. However, PSI animals accumulated high levels of CM cells more rapidly in GALT at an earlier time point in therapy than CSI animals. This is in agreement with previous studies reporting a correlation between preservation of CM $CD4^+$ T cells in peripheral blood of HIV-infected patients or vaccinated SIV-infected macaques with protection from disease (32, 42). We have previously determined that low-level viral replication in the GALT can contribute to continued $CD4^+$ T-cell depletion by causing the CM pool to differentiate into effectors (71). Although CM $CD4^+$ T cells are more resistant to loss from SIV, a reduction in this pool occurs in SIV infection (8, 52, 71). Our findings suggest that early initiation of ART may lead to an overall improvement in the pathogenesis of the intestinal mucosa and thereby decrease the rate of transition of CM to EM. A continued loss of the EM pool could strain the remaining CM pool to provide effector $CD4^+$ T-cell replacements. Therapeutics with an ability to enhance the recruitment or differentiation of CM $CD4^+$ T cells in human GALT during the initial stages of HAART may prove to be more effective in promoting gut mucosal immune restoration.

The $CD8^+$ T-cell responses observed in the PSI animals were very different from those observed in the CSI animals or SIV-infected untreated controls. SIV gag-specific $CD8^+$ T-cell responses in GALT of PSI were dominated by the single IL-2 expression after 6 weeks of ART that coincided with the start of restoration of $CD4^+$ T cells in both peripheral blood and GALT. $CD8^+$ T cells producing IL-2 may have higher proliferative or survival potential than those that produce only IFN-γ. In addition, loss of IL-2-producing T cells is a characteristic of exhaustion during HIV infection (26, 39). Patients that receive IL-2 therapy in conjunction with HAART not only have slightly increased numbers of $CD4^+$ T cells but also exhibit an increase in the number of HIV-suppressive noncytolytic $CD8^+$ T cells (13, 27, 28, 39). $CCR5^+$ $CD8^+$ T cells have been associated with more cytolytic $CD57^+$ or activated $CD38^+$ effectors in HIV^+ patients, while dual-positive ($CCR5^+$ $CXCR4^+$) T cells have less cytolytic potential (28, 31, 49). The up-regulation of CXCR4 on intestinal $CD8^+$ T cells in PSI animals is additional evidence for less cytotoxic SIV-specific $CD8^+$ T cells (31, 48, 63). Since the proliferation of both $CD8^+$ and $CD4^+$ T-cell pools of the PSI group were lower at 16 weeks and 30 weeks of ART than that in the CSI or untreated groups, it is possible that IL-2 derived from $CD8^+$ T cells might have been used for $CD4^+$ T-cell proliferation in GALT. In $CD8^+$ T cells obtained from patients treated during the primary HIV infection, in vitro supplementation of IL-2 increased their proliferation but more importantly increased their resistance to apoptosis (72). The IL-2-expressing $CD8^+$ T cells may produce other cytokines, such as MIP-1β, perforin, or granzyme B, with polyfunctionality and may help suppress or eliminate the virus (5, 6, 54). These cells, with lower lytic capacity, may also not contribute to inflammation and cell activation observed in GALT. Although antigen-specific $CD8^+$ T-cell responses in PSI animals were generally lower than CSI or untreated controls in GALT, the quality of the response may be important in supporting the restoration of $CD4^+$ T cells and augmenting the effects of ART. It has been reported

that vaccinated animals that were protected from pathogenic SIV challenge developed early antigen-specific CD8+ T-cell responses dominated by single IFN-γ production that evolved into dominant single IL-2-producing responses in peripheral blood (15). This mirrored the development of the antiviral response in GALT of PSI animals. It is also possible that the antiviral responses are influenced by the level of viral replication, and IL-2 singly producing CD8+ T cells may not be as functional as the IFN-γ-producing ones (3). Nevertheless, there was a strong correlation of the generation of single IL-2-producing CD8+ T cells with CD4+ T-cell restoration in the PSI group, while these cells were not detected in the SIV-infected untreated controls. It will be important to further analyze the functional characteristics of the single IL-2-producing CD8+ T cells for their role in the antiviral response and the impact of the restored CD4+ T-cell help in shaping this response.

Previous HIV studies have shown that the magnitude of inflammation and immune activation is associated with reduced CD4+ T-cell restoration in GALT (21). In the SIV model, inflammatory gene expression in GALT during SIV infection is reduced during therapy compared to untreated controls (16, 17). We previously reported increased expression of genes regulating inflammation and immune activation in GALT during HIV and SIV infection based on DNA microarray analysis (16–18, 21, 22). Based on this information, we used a panel of six inflammatory genes that are commonly dysregulated in SIV-infected untreated rhesus macaques to measure the degree of inflammation in our study. CSI animals had higher levels of inflammation-related gene transcription during ART than PSI animals. Increased expression of TGF-β, IL-8, and MIG in CSI animals suggested that the inflammation could be due, in part, to monocyte recruitment to GALT (66). Monocytes from the periphery differentiating into macrophages in GALT may bring additional infected or susceptible cells, contributing to continued viral replication. The increased level of phospholipase A_2 possibly indicates that heightened immune activation is continuing in the CSI animals despite ART (69). Despite similar levels of the virus in GALT of PSI and CSI animals at 30 weeks of ART, PAP levels were significantly higher in CSI animals. This suggested that the persistence of immune activation in GALT during therapy might be independent of viral loads. The relatively stable expression of TNF-α in the CSI group during therapy also indicated that starting ART during the later stage of infection might have sustained chronic inflammation despite the viral suppression. While the difference between the PSI and CSI groups was not statistically significant, there was a clear trend for increased levels of inflammation in CSI animals. Increased expression levels of GRP-78, a marker of chronic intestinal inflammation, and HSP-78 were detected in the CSI animals and untreated SIV-infected controls, which further supported the idea that chronic inflammation in GALT may impair CD4+ T-cell restoration (16, 21, 22, 64).

It is possible that the potential for gut mucosal repair and regeneration may be impaired during the course of SIV infection due to the chronic inflammation and immune activation (7, 19). In African green monkeys with nonpathogenic SIV infection, intestinal CD4+ T cells were depleted following SIV infection but were replenished subsequently, and these animals remained clinically asymptomatic (20, 53). Our previous studies of long-term HIV-infected nonprogressors (LTNP) showed that a clinically asymptomatic status and lack of HIV disease correlated with the maintenance of gut mucosal CD4+ T cells and gene expression regulating mucosal repair and regeneration (61). Although severe CD4+ T-cell depletion in GALT may cause immune dysfunction and may be an important feature of viral pathogenesis, the major challenge in restoring CD4+ T cells may stem from the inability of the host to repair and regenerate the mucosal damage caused by the virus. It will be important to explore drug regimens that may stimulate and promote the repair and regeneration of gut mucosa through limiting inflammation as an adjunct to standard ART.

In summary, we present multiple lines of evidence that initiating therapy at a time point prior to the occurrence of severe enteropathic changes leads to improved CD4+ T-cell restoration and maintenance/regeneration of CM T-cell pools. In previously reported studies of patients with HAART initiated in the primary HIV infection, the gut mucosal CD4+ T-cell restoration was variable and warrants further study (22, 46, 47). In the SIV model, monkeys that restored their CD4+ T cells in GALT early did not progress to SAIDS and were determined to be LTNP (38). Initiation of ART early in SIV-infected animals may model the development of the asymptomatic infection course observed in LTNP animals. Most importantly, our study in the SIV model indicates that complete CD4+ T-cell restoration is possible in the GALT and that further evaluation of therapy during early infection may be warranted. The CD4+ T-cell restoration was linked to viral suppression and a reduced inflammatory profile, suggesting that prevention or control of the chronic inflammation may limit severe damage to the gut microenvironment and would facilitate better immune restoration during therapy.

ACKNOWLEDGMENTS

We thank Linda Hirst, Sona Santos, and the staff at the Northern California National Primate Research Center and Michael George, Elizabeth Reay, and Thomas Ndolo for their review of the manuscript.

This study was supported by grants from the National Institutes of Health (DK43183 and AI 43274).

REFERENCES

1. **Abel, K., D. M. Rocke, B. Chohan, L. Fritts, and C. J. Miller.** 2005. Temporal and anatomic relationship between virus replication and cytokine gene expression after vaginal simian immunodeficiency virus infection. J. Virol. **79:**12164–12172.
2. **Agace, W. W., A. I. Roberts, L. Wu, C. Greineder, E. C. Ebert, and C. M. Parker.** 2000. Human intestinal lamina propria and intraepithelial lymphocytes express receptors specific for chemokines induced by inflammation. Eur. J. Immunol. **30:**819–826.
3. **Akerele, T., G. Galatowicz, C. Bunce, V. Calder, W. A. Lynn, and S. Lightman.** 2006. Normalized CD8+ but not CD4+ lymphocyte IL-2 expression is associated with early treatment with highly active antiretroviral therapy. Clin. Immunol. **121:**191–197.
4. **Amyes, E., A. J. McMichael, and M. F. Callan.** 2005. Human CD4+ T cells are predominantly distributed among six phenotypically and functionally distinct subsets. J. Immunol. **175:**5765–5773.
5. **Betts, M. R., B. Exley, D. A. Price, A. Bansal, Z. T. Camacho, V. Teaberry, S. M. West, D. R. Ambrozak, G. Tomaras, M. Roederer, J. M. Kilby, J. Tartaglia, R. Belshe, F. Gao, D. C. Douek, K. J. Weinhold, R. A. Koup, P. Goepfert, and G. Ferrari.** 2005. Characterization of functional and phenotypic changes in anti-Gag vaccine-induced T cell responses and their role in protection after HIV-1 infection. Proc. Natl. Acad. Sci. USA **102:**4512–4517.
6. **Betts, M. R., M. C. Nason, S. M. West, S. C. De Rosa, S. A. Migueles, J. Abraham, M. M. Lederman, J. M. Benito, P. A. Goepfert, M. Connors, M. Roederer, and R. A. Koup.** 2006. HIV nonprogressors preferentially maintain highly functional HIV-specific CD8+ T cells. Blood **107:**4781–4789.

7. **Biancotto, A., J. C. Grivel, S. J. Iglehart, C. Vanpouille, A. Lisco, S. F. Sieg, R. Debernardo, K. Garate, B. Rodriguez, L. B. Margolis, and M. M. Lederman.** 2007. Abnormal activation and cytokine spectra in lymph nodes of people chronically infected with HIV-1. Blood **109:**4272–4279.
8. **Bostik, P., E. S. Noble, A. E. Mayne, L. Gargano, F. Villinger, and A. A. Ansari.** 2006. Central memory CD4 T cells are the predominant cell subset resistant to anergy in SIV disease resistant sooty mangabeys. AIDS **20:**181–188.
9. **Brenchley, J. M., T. W. Schacker, L. E. Ruff, D. A. Price, J. H. Taylor, G. J. Beilman, P. L. Nguyen, A. Khoruts, M. Larson, A. T. Haase, and D. C. Douek.** 2004. CD4$^+$ T cell depletion during all stages of HIV disease occurs predominantly in the gastrointestinal tract. J. Exp. Med. **200:**749–759.
10. **Campbell, J. J., K. E. Murphy, E. J. Kunkel, C. E. Brightling, D. Soler, Z. Shen, J. Boisvert, H. B. Greenberg, M. A. Vierra, S. B. Goodman, M. C. Genovese, A. J. Wardlaw, E. C. Butcher, and L. Wu.** 2001. CCR7 expression and memory T cell diversity in humans. J. Immunol. **166:**877–884.
11. **Centlivre, M., M. Sala, S. Wain-Hobson, and B. Berkhout.** 2007. In HIV-1 pathogenesis the die is cast during primary infection. AIDS **21:**1–11.
12. **Dandekar, S.** 2007. Pathogenesis of HIV in the gastrointestinal tract. Curr. HIV Res. AIDS Rep. **4:**10–15.
13. **Durier, C., C. Capitant, A. S. Lascaux, C. Goujard, E. Oksenhendler, I. Poizot-Martin, J. P. Viard, L. Weiss, E. Netzer, J. F. Delfraissy, J. P. Aboulker, and Y. Levy.** 2007. Long-term effects of intermittent interleukin-2 therapy in chronic HIV-infected patients (ANRS 048-079 trials). AIDS **21:** 1887–1897.
14. **Fritsch, R. D., X. Shen, G. P. Sims, K. S. Hathcock, R. J. Hodes, and P. E. Lipsky.** 2005. Stepwise differentiation of CD4 memory T cells defined by expression of CCR7 and CD27. J. Immunol. **175:**6489–6497.
15. **Genescà, M., T. Rourke, J. Li, K. Bost, B. Chohan, M. B. McChesney, and C. J. Miller.** 2007. Live attenuated lentivirus infection elicits polyfunctional simian immunodeficiency virus Gag-specific CD8$^+$ T cells with reduced apoptotic susceptibility in rhesus macaques that control virus replication after challenge with pathogenic SIVmac239. J. Immunol. **179:**4732–4740.
16. **George, M. D., E. Reay, S. Sankaran, and S. Dandekar.** 2005. Early antiretroviral therapy for simian immunodeficiency virus infection leads to mucosal CD4$^+$ T-cell restoration and enhanced gene expression regulating mucosal repair and regeneration. J. Virol. **79:**2709–2719.
17. **George, M. D., S. Sankaran, E. Reay, A. C. Gelli, and S. Dandekar.** 2003. High-throughput gene expression profiling indicates dysregulation of intestinal cell cycle mediators and growth factors during primary simian immunodeficiency virus infection. Virology **312:**84–94.
18. **George, M. D., D. Verhoeven, Z. McBride, and S. Dandekar.** 2006. Gene expression profiling of gut mucosa and mesenteric lymph nodes in simian immunodeficiency virus-infected macaques with divergent disease course. J. Med. Primatol. **35:**261–269.
19. **Goicoechea, M., D. M. Smith, L. Liu, S. May, A. R. Tenorio, C. C. Ignacio, A. Landay, and R. Haubrich.** 2006. Determinants of CD4$^+$ T cell recovery during suppressive antiretroviral therapy: association of immune activation, T cell maturation markers, and cellular HIV-1 DNA. J. Infect. Dis. **194:**29–37.
20. **Gordon, S. N., N. R. Klatt, S. E. Bosinger, J. M. Brenchley, J. M. Milush, J. C. Engram, R. M. Dunham, M. Paiardini, S. Klucking, A. Danesh, E. A. Strobert, C. Apetrei, I. V. Pandrea, D. Kelvin, D. C. Douek, S. I. Staprans, D. L. Sodora, and G. Silvestri.** 2007. Severe depletion of mucosal CD4$^+$ T cells in AIDS-free simian immunodeficiency virus-infected sooty mangabeys. J. Immunol. **179:**3026–3034.
21. **Guadalupe, M., E. Reay, S. Sankaran, T. Prindiville, J. Flamm, A. McNeil, and S. Dandekar.** 2003. Severe CD4$^+$ T-cell depletion in gut lymphoid tissue during primary human immunodeficiency virus type 1 infection and substantial delay in restoration following highly active antiretroviral therapy. J. Virol. **77:**11708–11717.
22. **Guadalupe, M., S. Sankaran, M. D. George, E. Reay, D. Verhoeven, B. L. Shacklett, J. Flamm, J. Wegelin, T. Prindiville, and S. Dandekar.** 2006. Viral suppression and immune restoration in the gastrointestinal mucosa of human immunodeficiency virus type 1-infected patients initiating therapy during primary or chronic infection. J. Virol. **80:**8236–8247.
23. **Harari, A., V. Dutoit, C. Cellerai, P. A. Bart, R. A. Du Pasquier, and G. Pantaleo.** 2006. Functional signatures of protective antiviral T-cell immunity in human virus infections. Immunol. Rev. **211:**236–254.
24. **Hirsch, V. M., and J. D. Lifson.** 2000. Simian immunodeficiency virus infection of monkeys as a model system for the study of AIDS pathogenesis, treatment, and prevention. Adv. Pharmacol. **49:**437–477.
25. **Hofmann-Lehmann, R., R. K. Swenerton, V. Liska, C. M. Leutenegger, H. Lutz, H. M. McClure, and R. M. Ruprecht.** 2000. Sensitive and robust one-tube real-time reverse transcriptase-polymerase chain reaction to quantify SIV RNA load: comparison of one- versus two-enzyme systems. AIDS Res. Hum. Retrovir. **16:**1247–1257.
26. **Kannanganat, S., C. Ibegbu, L. Chennareddi, H. L. Robinson, and R. R. Amara.** 2007. Multiple-cytokine-producing antiviral CD4 T cells are functionally superior to single-cytokine-producing cells. J. Virol. **81:**8468–8476.
27. **Kinter, A. L., S. M. Bende, E. C. Hardy, R. Jackson, and A. S. Fauci.** 1995. Interleukin 2 induces CD8$^+$ T cell-mediated suppression of human immunodeficiency virus replication in CD4$^+$ T cells and this effect overrides its ability to stimulate virus expression. Proc. Natl. Acad. Sci. USA **92:**10985–10989.
28. **Kobayashi, N., H. Takata, S. Yokota, and M. Takiguchi.** 2004. Down-regulation of CXCR4 expression on human CD8$^+$ T cells during peripheral differentiation. Eur. J. Immunol. **34:**3370–3378.
29. **Lanzavecchia, A., and F. Sallusto.** 2000. Dynamics of T lymphocyte responses: intermediates, effectors, and memory cells. Science **290:**92–97.
30. **Lanzavecchia, A., and F. Sallusto.** 2005. Understanding the generation and function of memory T cell subsets. Curr. Opin. Immunol. **17:**219–229.
31. **Le Priol, Y., D. Puthier, C. Lecureuil, C. Combadiere, P. Debre, C. Nguyen, and B. Combadiere.** 2006. High cytotoxic and specific migratory potencies of senescent CD8$^+$ CD57$^+$ cells in HIV-infected and uninfected individuals. J. Immunol. **177:**5145–5154.
32. **Letvin, N. L., J. R. Mascola, Y. Sun, D. A. Gorgone, A. P. Buzby, L. Xu, Z. Y. Yang, B. Chakrabarti, S. S. Rao, J. E. Schmitz, D. C. Montefiori, B. R. Barker, F. L. Bookstein, and G. J. Nabel.** 2006. Preserved CD4$^+$ central memory T cells and survival in vaccinated SIV-challenged monkeys. Science **312:**1530–1533.
33. **Letvin, N. L., S. S. Rao, V. Dang, A. P. Buzby, B. Korioth-Schmitz, D. Dombagoda, J. G. Parvani, R. H. Clarke, L. Bar, K. R. Carlson, P. A. Kozlowski, V. M. Hirsch, J. R. Mascola, and G. J. Nabel.** 2007. No evidence for consistent virus-specific immunity in simian immunodeficiency virus-exposed, uninfected rhesus monkeys. J. Virol. **81:**12368–12374.
34. **Leutenegger, C. M., J. Higgins, T. B. Matthews, A. F. Tarantal, P. A. Luciw, N. C. Pedersen, and T. W. North.** 2001. Real-time TaqMan PCR as a specific and more sensitive alternative to the branched-chain DNA assay for quantitation of simian immunodeficiency virus RNA. AIDS Res. Hum. Retrovir. **17:**243–251.
35. **Li, Q., L. Duan, J. D. Estes, Z. M. Ma, T. Rourke, Y. Wang, C. Reilly, J. Carlis, C. J. Miller, and A. T. Haase.** 2005. Peak SIV replication in resting memory CD4$^+$ T cells depletes gut lamina propria CD4$^+$ T cells. Nature **434:**1148–1152.
36. **Lifson, J. D., M. Piatak, Jr., A. N. Cline, J. L. Rossio, J. Purcell, I. Pandrea, N. Bischofberger, J. Blanchard, and R. S. Veazey.** 2003. Transient early post-inoculation anti-retroviral treatment facilitates controlled infection with sparing of CD4$^+$ T cells in gut-associated lymphoid tissues in SIVmac239-infected rhesus macaques, but not resistance to rechallenge. J. Med. Primatol. **32:**201–210.
37. **Lifson, J. D., J. L. Rossio, R. Arnaout, L. Li, T. L. Parks, D. K. Schneider, R. F. Kiser, V. J. Coalter, G. Walsh, R. J. Imming, B. Fisher, B. M. Flynn, N. Bischofberger, M. Piatak, Jr., V. M. Hirsch, M. A. Nowak, and D. Wodarz.** 2000. Containment of simian immunodeficiency virus infection: cellular immune responses and protection from rechallenge following transient postinoculation antiretroviral treatment. J. Virol. **74:**2584–2593.
38. **Ling, B., R. S. Veazey, M. Hart, A. A. Lackner, M. Kuroda, B. Pahar, and P. A. Marx.** 2007. Early restoration of mucosal CD4 memory CCR5 T cells in the gut of SIV-infected rhesus predicts long term non-progression. AIDS **21:**2377–2385.
39. **Martinez-Marino, B., S. Shiboski, F. M. Hecht, J. O. Kahn, and J. A. Levy.** 2004. Interleukin-2 therapy restores CD8 cell non-cytotoxic anti-HIV responses in primary infection subjects receiving HAART. AIDS **18:**1991–1999.
40. **Marzo, A. L., H. Yaquita, and L. Lefrançois.** 2007. Cutting edge: migration to nonlymphoid tissues results in functional conversion of central to effector memory CD8 T cells. J. Immunol. **179:**36–40.
41. **Mattapallil, J. J., D. C. Douek, B. Hill, Y. Nishimura, M. Martin, and M. Roederer.** 2005. Massive infection and loss of memory CD4$^+$ T cells in multiple tissues during acute SIV infection. Nature **434:**1093–1097.
42. **Mattapallil, J. J., D. C. Douek, A. Buckler-White, D. Montefiori, N. L. Letvin, G. J. Nabel, and M. Roederer.** 2006. Vaccination preserves CD4 memory T cells during acute simian immunodeficiency virus challenge. J. Exp. Med. **203:**1533–1541.
43. **Mattapallil, J. J., Z. Smit-McBride, P. Dailey, and S. Dandekar.** 1999. Activated memory CD4$^+$ T helper cells repopulate the intestine early following antiretroviral therapy of simian immunodeficiency virus-infected rhesus macaques but exhibit a decreased potential to produce interleukin-2. J. Virol. **73:**6661–6669.
44. **McGowan, I., J. Elliott, M. Fuerst, P. Taing, J. Boscardin, M. Poles, and P. Anton.** 2004. Increased HIV-1 mucosal replication is associated with generalized mucosal cytokine activation. J. Acquir. Immune Defic. Syndr. **37:** 1228–1236.
45. **Mehandru, S., and S. Dandekar.** 2008. Role of the gastrointestinal tract in establishing infection in primates and humans. Curr. Opin. HIV AIDS **3:**22–27.
46. **Mehandru, S., M. A. Poles, K. Tenner-Racz, P. Jean-Pierre, V. Manuelli, P. Lopez, A. Shet, A. Low, H. Mohri, D. Boden, P. Racz, and M. Markowitz.** 2006. Lack of mucosal immune reconstitution during prolonged treatment of acute and early HIV-1 infection. PLoS Med. **3:**e484.
47. **Mehandru, S., M. A. Poles, K. Tenner-Racz, V. Manuelli, P. Jean-Pierre, P. Lopez, A. Shet, A. Low, H. Mohri, D. Boden, P. Racz, and M. Markowitz.** 2007. Mechanisms of gastrointestinal CD4+ T cell depletion during acute and early HIV-1 infection. J. Virol. **81:**599–612.
48. **Monceaux, V., L. Viollet, F. Petit, R. Ho Tsong Fang, M. C. Cumont, J.**

Zaunders, B. Hurtrel, and J. Estaquier. 2005. CD8+ T cell dynamics during primary simian immunodeficiency virus infection in macaques: relationship of effector cell differentiation with the extent of viral replication. J. Immunol. **174:**6898–6908.

49. **Nicholson, J. K., S. W. Browning, R. L. Hengel, E. Lew, L. E. Gallagher, D. Rimland, and J. S. McDougal.** 2001. CCR5 and CXCR4 expression on memory and naive T cells in HIV-1 infection and response to highly active antiretroviral therapy. J. Acquir. Immune Defic. Syndr. **27:**105–115.
50. **Nilsson, J., S. Kinloch-de-Loes, A. Granath, A. Sönnerborg, L. E. Goh, and J. Andersson.** 2007. Early immune activation in gut-associated and peripheral lymphoid tissue during acute HIV infection. AIDS **21:**5.
51. **Nowak, M. A., A. L. Lloyd, G. M. Vasquez, T. A. Wiltrout, L. M. Wahl, N. Bischofberger, J. Williams, A. Kinter, A. S. Fauci, V. M. Hirsch, and J. D. Lifson.** 1997. Viral dynamics of primary viremia and antiretroviral therapy in simian immunodeficiency virus infection. J. Virol. **71:**7518–7525.
52. **Okoye, A., M. Meier-Schellersheim, J. M. Brenchley, S. I. Hagen, J. M. Walker, M. Rohankhedkar, R. Lum, J. B. Edgar, S. L. Planer, A. Legasse, A. W. Sylwester, M. Piatak, Jr., J. D. Lifson, V. C. Maino, D. L. Sodora, D. C. Douek, M. K. Axthelm, Z. Grossman, and L. J. Picker.** 2007. Progressive CD4+ central memory T cell decline results in CD4+ effector memory insufficiency and overt disease in chronic SIV infection. J. Exp. Med. **204:** 2171–2185.
53. **Pandrea, I. V., R, Gautam, R. M. Ribeiro, J. M. Brenchley, I. F. Butler, M. Pattison, T. Rasmussen, P. A. Marx, G. Silvestri, A. A. Lackner, A. S. Perelson, D. C. Douek, R. S. Veazey, and C. Apetrei.** 2007. Acute loss of intestinal CD4+ T cells is not predictive of simian immunodeficiency virus virulence. J. Immunol. **179:**3035–3046.
54. **Peretz, Y., M. L. Ndongala, S. Boulet, M. R. Boulassel, D. Rouleau, P. Cote, D. Longpre, J. P. Routy, J. Falutz, C. Tremblay, C. M. Tsoukas, R. P. Sekaly, and N. F. Bernard.** 2007. Functional T cell subsets contribute differentially to HIV peptide-specific responses within infected individuals: correlation of these functional T cell subsets with markers of disease progression. Clin. Immunol. **124:**57–68.
55. **Picker, L.** 2006. Immunopathogenesis of acute AIDS virus infection. Curr. Opin. Immunol. **18:**399–405.
56. **Picker, L. J., E. F. Reed-Inderbitzin, S. I. Hagen, J. B. Edgar, S. G. Hansen, A. Legasse, S. Planer, M. Piatak, Jr., J. D. Lifson, V. C. Maino, M. K. Axthelm, and F. Villinger.** 2006. IL-15 induces CD4 effector memory T cell production and tissue emigration in nonhuman primates. J. Clin. Investig. **116:**1514–1524.
57. **Pitcher, C. J., S. I. Hagen, J. M. Walker, R. Lum, B. L. Mitchell, V. C. Maino, M. K. Axthelm, and L. J. Picker.** 2002. Development and homeostasis of T cell memory in rhesus macaque. J. Immunol. **168:**29–43.
58. **Poonia, B., S. Nelson, G. J. Bagby, and R. S. Veazey.** 2006. Intestinal lymphocyte subsets and turnover are affected by chronic alcohol consumption: implications for SIV/HIV infection. J. Acquir. Immune Defic. Syndr. **41:**537–547.
59. **Poonia, B., L. Walter, J. Dufour, R. Harrison, P. A. Marx, and R. S. Veazey.** 2006. Cyclic changes in the vaginal epithelium of normal rhesus macaques. J. Endocrinol. **190:**829–835.
60. **Precopio, M. L., M. R. Betts, J. Parrino, D. A. Price, E. Gostick, D. R. Ambrozak, T. E. Asher, D. C. Douek, A. Harari, G. Pantaleo, R. Bailer, B. S. Graham, M. Roederer, and R. A. Koup.** 2007. Immunization with vaccinia virus induces polyfunctional and phenotypically distinctive CD8+ T cell responses. J. Exp. Med. **204:**1405–1416.
61. **Sankaran, S., M. Guadalupe, E. Reay, M. D. George, J. Flamm, T. Prindiville, and S. Dandekar.** 2005. Gut mucosal T cell responses and gene expression correlate with protection against disease in long-term HIV-1-infected nonprogressors. Proc. Natl. Acad. Sci. USA **102:**9860–9865.
62. **Schaefer, T. M., C. L. Fuller, S. Basu, B. A. Fallert, S. L. Poveda, S. K. Sanghavi, Y. K. Choi, D. E. Kirschner, E. Feingold, and T. A. Reinhart.** 2000. Increased expression of interferon-inducible genes in macaque lung tissues during simian immunodeficiency virus infection. Microbes Infect. **8:**1839–1850.
63. **Shacklett, B. L., C. A. Cox, J. K. Sandberg, N. H. Stollman, M. A. Jacobson, and D. F. Nixon.** 2003. Trafficking of human immunodeficiency virus type 1-specific CD8+ T cells to gut-associated lymphoid tissue during chronic infection. J. Virol. **77:**5621–5631.
64. **Shkoda, A., P. A. Ruiz, H. Daniel, S. C. Kim, G. Rogler, R. B. Sartor, and D. Haller.** 2007. Interleukin-10 blocked endoplasmic reticulum stress in intestinal epithelial cells: impact on chronic inflammation. Gastroenterology **132:** 190–207.
65. **Smith, M. S., L. Foresman, G. J. Lopez, J. Tsay, D. Wodarz, J. D. Lifson, A. Page, C. Wang, Z. Li, I. Adany, S. Buch, N. Bischofberger, and O. Narayan.** 2000. Lasting effects of transient postinoculation tenofovir [9-R-(2-Phosphonomethoxypropyl)adenine] treatment on SHIV(KU2) infection of rhesus macaques. Virology **277:**306–315.
66. **Smythies, L. E., A. Maheshwari, R. Clements, D. Eckhoff, L. Novak, H. L. Vu, L. M. Mosteller-Barnum, M. Sellers, and P. D. Smith.** 2006. Mucosal IL-8 and TGF-beta recruit blood monocytes: evidence for cross-talk between the lamina propria stroma and myeloid cells. J. Leukoc. Biol. **80:**492–499.
67. **Song, K., R. L. Rabin, B. J. Hill, S. C. De Rosa, S. P. Perfetto, H. H. Zhang, J. F. Foley, J. S. Reiner, J. Liu, J. J. Mattapallil, D. C. Douek, M. Roederer, and J. M. Farber.** 2005. Characterization of subsets of CD4+ memory T cells reveals early branched pathways of T cell differentiation in humans. Proc. Natl. Acad. Sci. USA **102:**7916–7921.
68. **Stone, J. D., C. C. Heise, C. J. Miller, C. H. Halsted, and S. Dandekar.** 1994. Development of malabsorption and nutritional complications in simian immunodeficiency virus-infected rhesus macaques. AIDS **8:**1245–1256.
69. **Sturm, A., and A. U. Dignass.** 2002. Modulation of gastrointestinal wound repair and inflammation by phospholipids. Biochim. Biophys. Acta **1582:** 282–288.
70. **Veazey, R. S., K. G. Mansfield, I. C. Tham, A. C. Carville, D. E. Shvetz, A. E. Forand, and A. A. Lackner.** 2000. Dynamics of CCR5 expression by CD4+ T cells in lymphoid tissues during simian immunodeficiency virus infection. J. Virol. **74:**11001–11007.
71. **Verhoeven, D., S. Sankaran, and S. Dandekar.** 2007. Simian immunodeficiency virus infection induces severe loss of intestinal central memory T cells which impairs CD4+ T-cell restoration during antiretroviral therapy. J. Med. Primatol. **36:**219–227.
72. **Zaunders, J. J., L. Moutouh-de Parseval, S. Kitada, J. C. Reed, S. Rought, D. Genini, L. Leoni, A. Kelleher, D. A. Cooper, D. E. Smith, P. Grey, J. Estaquier, S. Little, D. D. Richman, and J. Corbeil.** 2003. Polyclonal proliferation and apoptosis of CCR5+ T lymphocytes during primary human immunodeficiency virus type 1 infection: regulation by interleukin (IL)-2, IL-15, and Bcl-2. J. Infect. Dis. **187:**1735–1747.
73. **Zimmerli, S. C., A. Harari, C. Cellerai, F. Vallelian, P. A. Bart, and G. Pantaleo.** 2005. HIV-1-specific IFN-gamma/IL-2-secreting CD8 T cells support CD4-independent proliferation of HIV-1-specific CD8 T cells. Proc. Natl. Acad. Sci. USA **102:**7239–7244.